

Triangular-spin, kagome plane in jarosites

M. G. Townsend*

Department of Energy, Mines and Resources, Ottawa, Ontario, Canada

G. Longworth

Atomic Energy Research Establishment, Harwell, United Kingdom

E. Roudaut

Centre d'Etudes Nucleaires de Grenoble, Grenoble, France

(Received 19 July 1985; revised manuscript received 3 December 1985)

Iron atoms in $\text{KFe}_3(\text{OH})_6(\text{SO}_4)_2$ and related jarosite-type materials occur in kagome planes separated by about 5.7 Å. A planar magnetic interaction is indicated from magnetic-susceptibility and neutron diffraction measurements. Triangular-spin antiferromagnetic ordering ($T_N = 46$ and 65 K) is observed in $\text{KFe}_3(\text{OH})_6(\text{SO}_4)_2$, and $\text{KFe}_3(\text{OH})_6(\text{CrO}_4)_2$, respectively, from powder neutron diffraction, Mössbauer, and magnetic-susceptibility data. The magnetic cell of $\text{KFe}_3(\text{OH})_6(\text{SO}_4)_2$ is double that of the crystallographic cell along the *c*-axis direction, while in $\text{KFe}_3(\text{OH})_6(\text{CrO}_4)_2$ the two cells are identical. A weak moment of $0.03\mu_B/(\text{Fe atom})$ occurs at temperatures below 65 K, the antiferromagnetic ordering temperature, in $\text{KFe}_3(\text{OH})_6(\text{CrO}_4)_2$. The susceptibilities of $\text{KCr}_3(\text{OH})_6(\text{SO}_4)_2$, a new material, follow a Curie-Weiss law above 20 K. Below this temperature the susceptibilities suggest ordering at 1–2 K. Triangular-spin configurations follow by the application of Bertaut's matrix method to the kagome lattice. Superexchange (134°) is stronger by more than an order of magnitude in $\text{KFe}_3(\text{OH})_6(\text{SO}_4)_2$ and $\text{KFe}_3(\text{OH})_6(\text{CrO}_4)_2$ than in $\text{KCr}_3(\text{OH})_6(\text{SO}_4)_2$. Comparison is made with Fe_2O_3 and Cr_2O_3 .

I. INTRODUCTION

The synthesis of several jarosites, $M\text{Fe}_3(\text{OH})_6(\text{SO}_4)_2$, where *M* is H_3O^+ , Na^+ , K^+ , Rb^+ , Ag^+ , NH_4^+ , Tl^+ , Pb^{2+} , or Hg^{2+} , has recently been reported by Dutrizac and Kaiman.¹ Earlier studies had been described by Kubisz.² A chromate analog of jarosite, $\text{KFe}_3(\text{OH})_6(\text{CrO}_4)_2$, is also known.³

The crystal structure of jarosite $\text{KFe}_3(\text{OH})_6(\text{SO}_4)_2$ is related to that of alunite.^{4–6} The space group is $R\bar{3}m$, although nonstoichiometry, in particular, partial substitution of H_3O^+ for K^+ , means that $R\bar{3}m$ might strictly be more appropriate.⁶ All iron atoms in the structure are crystallographically equivalent and coordinated by two oxygen atoms and four hydroxyl groups. In the crystal *c* plane, Fe atoms form a kagome lattice (Fig. 1).^{5,7,8} Neighboring iron octahedra share an OH corner in common and the principal magnetic exchange in the kagome plane is superexchange via the $134^\circ \text{Fe}^{3+}-\text{OH}-\text{Fe}^{3+}$ bond angle. The shortest distance between Fe atoms in adjacent kagome planes is 6.3 Å. However, there is no obvious direct superexchange path. The available paths, $\text{Fe}-\text{O}-\text{S}-\text{O}-\text{OH}-\text{Fe}$ or $\text{Fe}-\text{OH}-\text{K}-\text{OH}-\text{Fe}$, both contain some rather large bond distances between adjacent atoms. A pronounced two-dimensional character is therefore expected for the magnetic properties.

Takano *et al.*⁸ have reported magnetic susceptibility data on $\text{KFe}_3(\text{OH})_6(\text{SO}_4)_2$. They deduced from the absence of metamagnetism and the negative sign of the Curie-Weiss constant Θ that each kagome plane is itself a

compensated antiferromagnet.

There have been a number of Mössbauer experiments on jarosites^{9–11} and magnetic ordering at low temperature has been confirmed. From their Mössbauer spectra, Takano *et al.*⁹ speculated that the spins of iron atoms in the kagome plane form triangular magnetic structures.

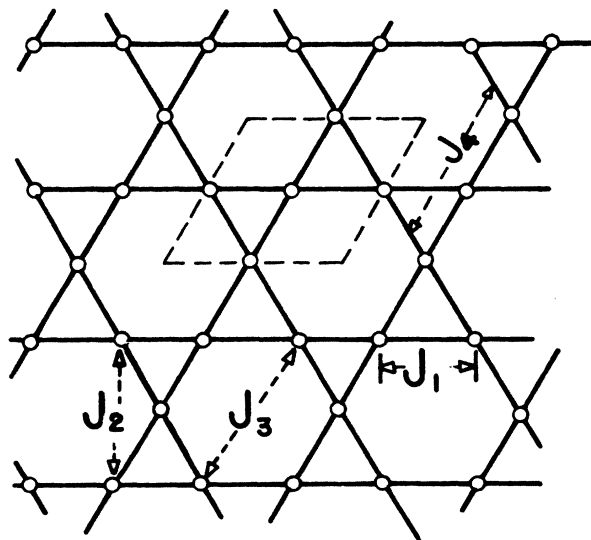


FIG. 1. Kagome plane, with iron positions, unit cell in *c* plane and principal magnetic exchange interactions, J_1 , J_2 , J_3 , J_4 in the plane.

In the present work neutron diffraction data have been recorded at 4 K to determine the magnetic structures of $\text{KFe}_3(\text{OH})_6(\text{SO}_4)_2$ and $\text{KFe}_3(\text{OH})_6(\text{CrO}_4)_2$. Magnetic susceptibility and Mössbauer data have also been recorded on these materials and magnetic susceptibility data on $\text{KCr}_3(\text{OH})_6(\text{SO}_4)_2$, a new material, are reported.

II. EXPERIMENTAL

The materials used in this work were synthesized by Dutrizac. Detailed descriptions of the synthesis of related materials have been reported earlier.¹ Reagent-grade chemicals were used for all the syntheses which were carried out in the presence of air. The potassium jarosite was prepared by reacting 1 l of 0.2M $\text{Fe}(\text{SO}_4)_{1.5}$ —0.3M K_2SO_4 solution at 140°C for 24 h in a Parr 2-l autoclave. Titanium autoclave internals were used together with a glass liner; the solution was stirred at 600 rpm. The pH was initially adjusted to 1.6 with $\text{Li}_2\text{CO}_3/\text{H}_2\text{SO}_4$ and allowed to fall during the precipitation of the jarosite. At the completion of the test, the slurry was filtered hot, washed with copious quantities of hot water, and dried at 110°C. X-ray powder-diffraction analysis showed the product, a pale yellow in color, to be single-phase potassium jarosite containing (in wt. %): 7.68 K, 29.87 Fe, and 39.45 SO_4 (theoretical composition: 7.81 K, 33.45 Fe, and 38.36 SO_4). A deficiency of K and Fe seems to be characteristic of jarosite-type compounds. Allowing the Fe occupancy factor to float in the fit to the neutron diffraction data yielded results in close agreement to the above.

The chromate analogue $[\text{KFe}_3(\text{CrO}_4)_2(\text{OH})_6]$ of potassium jarosite was synthesized by reacting 1 l of 0.2M $\text{Fe}(\text{NO}_3)_3$ —0.2M K_2CrO_4 solution at 98°C for 24 h in a well-stirred reaction kettle. The solution pH was initially adjusted to 1.5 with HNO_3 and the pH fell during the course of the hydrolysis reaction. At the completion of the test, the slurry was filtered hot, washed with hot water, and then dried at 110°C. The product was orange in color and shown by x-ray powder-diffraction analysis to consist of a single-phase jarosite-type compound whose composition was (in wt. %): 6.75 K, 29.47 Fe, 43.28 CrO_4 , 0.0 SO_4 (theoretical composition: 7.23 K, 30.99 Fe, 42.91 CrO_4). In this material, chromium occurs as Cr(VI), d^0 , and is diamagnetic.

A new material $\text{KCr}_3(\text{OH})_6(\text{SO}_4)_2$, a bright green in color, has also been synthesized.¹² X-ray powder-diffraction analysis showed the product to be a single-phase jarosite-type compound. Here chromium is trivalent, d^3 .

Powder neutron diffraction data were recorded on the multidetector powder diffractometer in the Siloe reactor at the Centre d'Etudes Nucleaires de Grenoble at 10 K and 80 K with a wavelength of 2.478. Earlier neutron diffraction data had been recorded on K^+ , Tl^+ , $\frac{1}{2}\text{Pb}^{2+}$ jarosites at the McMaster University reactor using a wavelength of 1.39 Å by Collins.¹³

Mössbauer spectra were recorded on a conventional spectrometer with a constant-acceleration drive at temperatures between 4 and 300 K. Spectra were computer fitted by a least-squares, iterative procedure. Magnetic

susceptibilities of powdered jarosites were recorded by Muir¹⁴ with a commercial vibrating sample magnetometer and associated cryostat at temperatures between 2 and 300 K. The equipment and method of measurement have been described elsewhere.¹⁵

III. RESULTS

The neutron diffraction patterns of $\text{KFe}_3(\text{OH})_6(\text{SO}_4)_2$ and $\text{KFe}_3(\text{OH})_6(\text{CrO}_4)_2$ at 10 K and at 80 K are shown in Figs. 2 and 3, respectively. The reflections are indexed at 10 K on a unit cell for $\text{KFe}_3(\text{OH})_6(\text{SO}_4)_2$ of $a=7.30$ Å and $c=17.09$ Å, and for $\text{KFe}_3(\text{OH})_6(\text{CrO}_4)_2$ of $a=7.4$ Å and $c=17.4$ Å. The reflection indices show that the size of the magnetic cell of $\text{KFe}_3(\text{OH})_6(\text{SO}_4)_2$ is twice that of the chemical unit cell in the c -axis direction, whereas the magnetic and chemical unit cells in $\text{KFe}_3(\text{OH})_6(\text{CrO}_4)_2$ are identical. The magnetic reflections $(1,0,\frac{1}{2})$, $(0,1,\frac{1}{2})$, $(1,0,\frac{7}{2})$, $(1,1,\frac{3}{2})$, $(0,1,\frac{11}{2})$, $(1,1,\frac{9}{2})$, $(1,0,\frac{13}{2})$, $(2,1,\frac{1}{2})$, $(2,1,\frac{7}{2})$ for $\text{KFe}_3(\text{OH})_6(\text{SO}_4)_2$ and the mixed magnetic-nuclear reflections, $(1,0,1)$, $(0,1,2)$, $(1,1,0)$, $(1,0,4)$, $(0,1,5)$, $(1,2,2)$, $(1,1,3)$, $(1,2,2)$, $(1,0,7)$, $(1,1,6)$, $(2,1,4)$ for $\text{KFe}_3(\text{OH})_6(\text{CrO}_4)_2$ indicate triangular-spin configuration.

The data for $\text{KFe}_3(\text{OH})_6(\text{SO}_4)_2$ were fitted by integrating the intensities of nine magnetic and 12 nuclear reflections separately followed by computer fitting to a structural model. Initial atomic positions and anisotropic thermal parameters were taken from Refs. 4 and 5. A nine-parameter nuclear fit was used. Potassium and iron are in special positions and eight positional parameters were evaluated from the data at 10 K yielding the following.

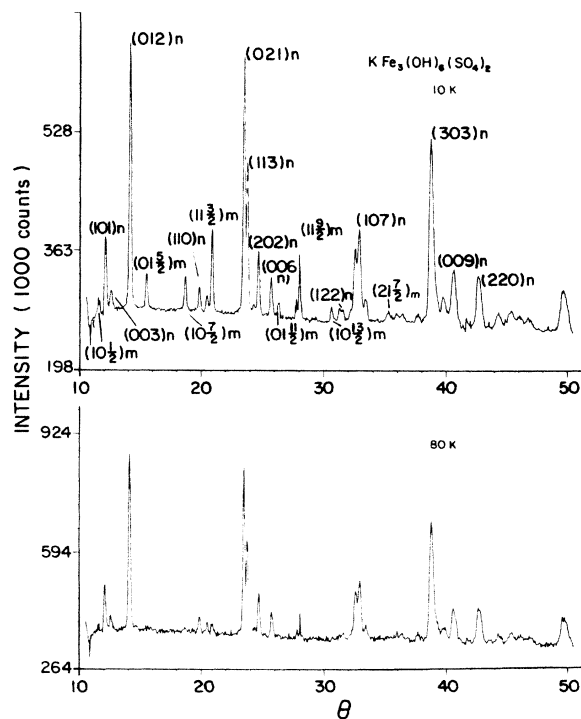


FIG. 2. Powder neutron diffraction pattern of $\text{KFe}_3(\text{OH})_6(\text{SO}_4)_2$ at 10 and 80 K, indexed at 10 K on a cell $a=7.30$ Å, $c=17.09$ Å. Magnetic reflections indicated by m , nuclear reflections by n .

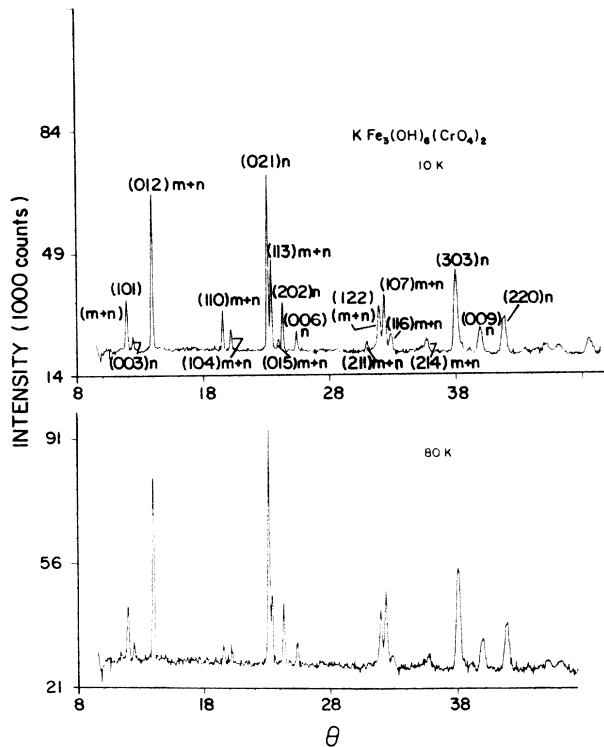


FIG. 3. Powder neutron diffraction of $\text{KFe}_3(\text{OH})_6(\text{CrO}_4)_2$ at 10 and 80 K, indexed at 10 K on a cell $a=7.4 \text{ \AA}$, $c=17.4 \text{ \AA}$. Magnetic reflections indicated by m , nuclear reflections by n .

	a_1	a_2	c
Sulfur	0.0	0.0	0.276
Oxygen (1)	0.0	0.0	0.407
Oxygen (2)	0.223	-0.233	-0.040
Oxygen (H)	0.133	-0.133	0.128
Hydrogen	0.191	-0.191	0.107

In $\text{KFe}_3(\text{OH})_6(\text{CrO}_4)_2$ a difference pattern was initially obtained from 10- and 80-K data followed by integration of the magnetic peaks.

In the magnetic fits, three spin directions, mutually at 120° to each other, were chosen at the Fe atoms located at $(\frac{1}{2}, 0, \frac{1}{2})$, $(\frac{1}{2}, \frac{1}{2}, \frac{1}{2})$, and $(0, \frac{1}{2}, \frac{1}{2})$. These three spin directions were taken in the zx , xy , or yz planes (Cartesian coordinates). For the spin directions at the remaining six Fe atoms all combinations and permutations of the three spin directions were tried. In addition, in the xy (and zx and yz) plane, the x and y components were interchanged giving in all 216 different permutations. In some fits, for both potassium jarosite and the chromate analogue the triangle of spins at $\frac{1}{6}c$ (and at $\frac{5}{6}c$) was rotated about the c axis with respect to the spins at $\frac{1}{2}c$, with the angle of rotation being allowed to float.

The spins were reversed in the second half of the doubled magnetic cell of potassium jarosite. Fits were also made to models in which the spins were rotated by π in the second half of the cell. A fit of the data of $\text{KFe}_3(\text{OH})_6(\text{SO}_4)_2$ to a theoretical model is shown in Fig. 4.

The best magnetic spin structures were found with the spins perpendicular to c for the two jarosites, and these models are shown in Figs. 5 and 6. The doubling of the unit cell for $\text{KFe}_3(\text{OH})_6(\text{SO}_4)_2$ is not indicated in Fig. 5.

The fit for $\text{KFe}_3(\text{OH})_6(\text{SO}_4)_2$ gives an Fe^{3+} moment of $4.3\mu_B$ with a nuclear R value of 2%, and a magnetic R value of 10%. The fit to the data of $\text{KFe}_3(\text{OH})_6(\text{CrO}_4)_2$, yields an Fe^{3+} moment of $3.7\mu_B$ with R magnetic equal to 20%. Two or three other triangular-spin models closely related to those shown in Figs. 5 and 6 cannot be ruled out since they give in some cases an almost comparable fit: $R > 1.1R_{\text{min}}$. Fits by Collins¹³ to neutron diffraction data on $\text{TlFe}_3(\text{OH})_6(\text{SO}_4)_2$ and $\text{PbFe}_6(\text{OH})_{12}(\text{SO}_4)_4$ indicate a magnetic structure similar to that of $\text{KFe}_3(\text{OH})_6(\text{SO}_4)_2$.

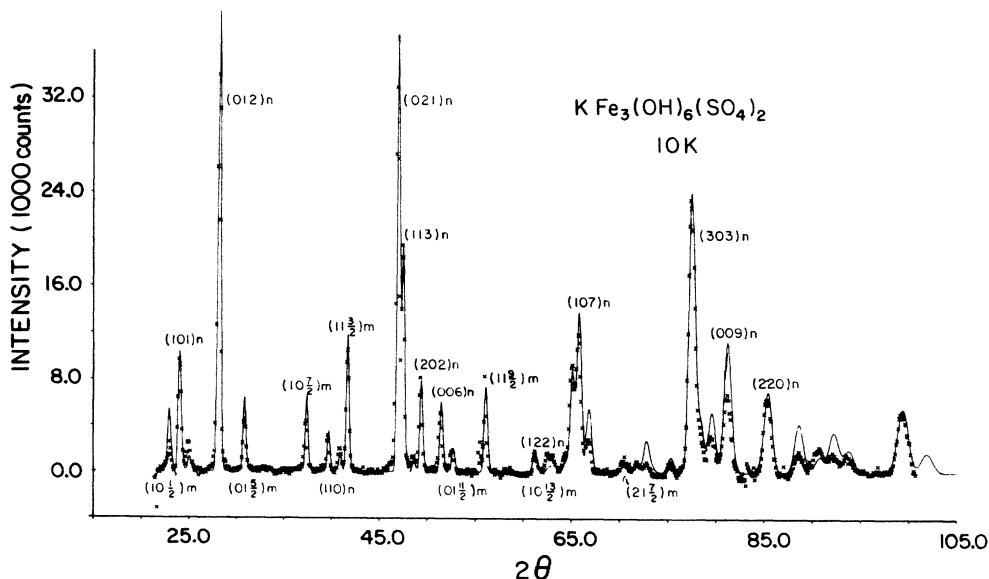


FIG. 4. Fit of theoretical model to experimental $\text{KFe}_3(\text{OH})_6(\text{SO}_4)_2$ neutron diffraction data at 10 K.

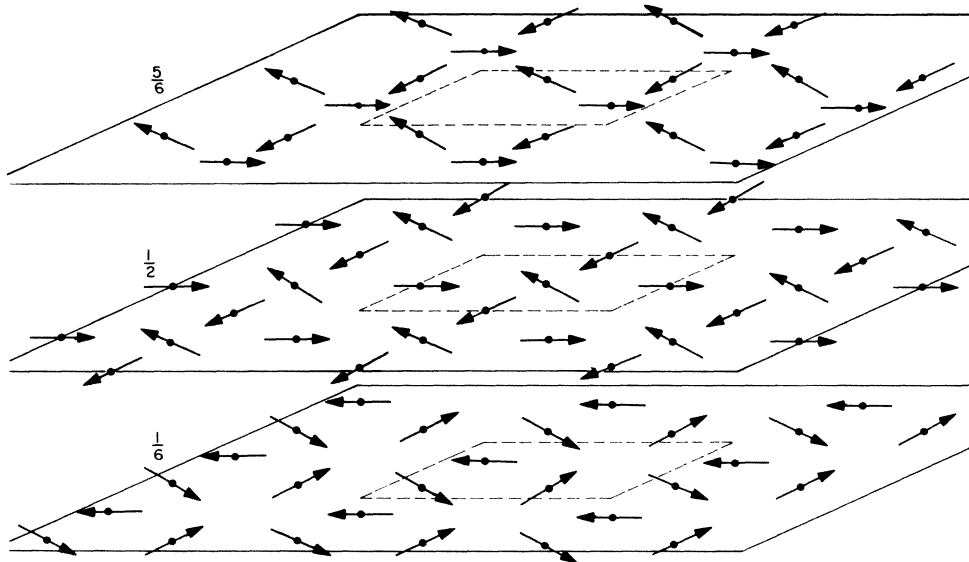


FIG. 5. Spin directions at Fe atoms of the three kagome planes of the hexagonal crystallographic unit cell of $\text{KFe}_3(\text{OH})_6(\text{SO}_4)_2$. Dashed lines indicate the unit cell. The magnetic cell is doubled: Reversed spin directions in the second half of the magnetic cell are not shown.

Mössbauer spectra of $\text{KFe}_3(\text{OH})_6(\text{SO}_4)_2$ recorded at 4 K are similar to those reported earlier.⁹ At 4 K, $H=490$ kOe, $\frac{1}{2}e^2qQ$ (quadrupole splitting) = 1.15 mm s^{-1} . S_I (isomer shift) = 0.49 relative to Fe metal, θ (angle between principle axis of electric-field gradient tensor and H , the internal magnetic field) = 90° , $\eta=0$. In this fit the quadrupole asymmetry parameter, η , was fixed at zero and all other parameters were allowed to float. Mössbauer spectra of $\text{KFe}_3(\text{OH})_6(\text{CrO}_4)_2$ as a function of temperature are shown in Fig. 7. At 10 K, $H=478$ kOe, $\frac{1}{2}e^2qQ=0.80$,

$S_I=0.47$ relative to Fe metal, $\theta=90^\circ$, and $\eta=0$. An approximate fit of the magnetic hyperfine-field splitting (H) data to a Brillouin curve with $S=\frac{5}{2}$ is shown in Fig. 8; the planar nature of the magnetism is shown by the steeper fall in hyperfine field close to T_N . T_N for $\text{KFe}_3(\text{OH})_6(\text{CrO}_4)_2$ was evaluated as 65 K from Fig. 7.

In an external magnetic field of 42 kOe the magnetic-hyperfine components in the spectrum of $\text{KFe}_3(\text{OH})_6(\text{CrO}_4)_2$ broaden indicating predominant antiferromagnetism [Figs. 9(a) and 9(b)]. Magnetic-

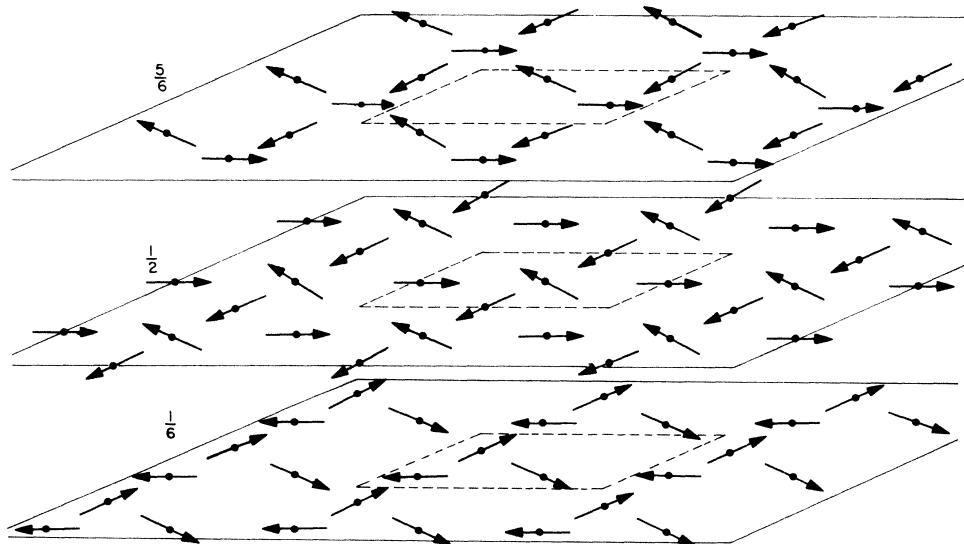


FIG. 6. Spin directions in the three kagome planes of the magnetic cell of $\text{KFe}_3(\text{OH})_6(\text{CrO}_4)_2$. Dashed lines indicate the unit cell.

susceptibility data on $\text{KFe}_3(\text{OH})_6(\text{SO}_4)_2$ as a function of temperature¹³ are similar to results of Takano.⁸ A broad peak at 46 K indicates the onset of three-dimensional magnetic ordering. Takano⁸ fitted his data to $\chi = C/(T - \Theta)$ with $\Theta = -600$ K and with an effective moment equal to the free-ion value for Fe^{3+} ($6\mu_B$). Muir's results are close to these.¹⁴

From the magnetic susceptibilities of $\text{KFe}_3(\text{OH})_6(\text{CrO}_4)_2$ (Ref. 14) at temperatures above 65 K, $\Theta = -600$ K and the effective moment for Fe^{3+} is $5.5\mu_B$. At 65 K the susceptibility rises infinitely indicating a spontaneous moment. This temperature coincides within experimental error to the temperature of onset of three-dimensional antiferromagnetic ordering as shown by Mössbauer spectroscopy, Fig. 7. The spontaneous moment has a value of $0.03\mu_B$ per Fe atom at 0 K, $M(0)$. Its temperature dependence is compared to that of the magnetic-hyperfine field splitting, H , with $M(0)$ normalized to $H(0)$, in Fig. 8.

Magnetic susceptibility data of $\text{KCr}_3(\text{OH})_6(\text{SO}_4)_2$ (Ref. 14) are shown in Fig. 10. The linear part of the χ^{-1} vs T curve is fitted to a Curie-Weiss law with $\Theta = -67.5$ and with an effective moment of $3.7\mu_B$ close to the free-ion value for Cr^{3+} of $3.87\mu_B$; the experimental range of values observed for Cr^{3+} are generally $(3.7-3.9)\mu_B$. We have assumed 100% occupancy for Cr^{3+} in the jarosite lattice. At very low temperature the curve in susceptibility data suggests magnetic ordering at $T_N \approx 1-2$ K.

IV. MAGNETIC STRUCTURE, THEORETICAL DEVELOPMENT

We derive a triangular-spin structure in the kagome plane of the jarosite using the matrix method of Bertaut.¹⁶ For simplicity we consider exchange interaction in one kagome plane only.

The three magnetic ions in the chemical unit cell, in a kagome plane (Fig. 1), form three Bravais lattices. The interaction matrix has the form

$$\xi(k) = \begin{pmatrix} A & B & C \\ B & A' & D \\ C & D & A'' \end{pmatrix},$$

where

$$A = 2J_3 \cos(2\pi k) + 2J_4 \cos(2\pi h) + 2J_4 \cos[2\pi(h+k)],$$

$$A' = 2J_3 \cos[2\pi(h+k)] + 2J_4 \cos(2\pi h) + 2J_4 \cos(2\pi k),$$

$$A'' = 2J_3 \cos(2\pi h) + 2J_4 \cos(2\pi k) + 2J_4 \cos[2\pi(h+k)],$$

$$B = 2J_1 \cos(\pi h) + 2J_2 [\cos \pi(h+2k)],$$

$$C = 2J_1 \cos[\pi(h+k)] + 2J_2 \cos[\pi(h-k)],$$

$$D = 2J_1 \cos(\pi k) + 2J_2 \cos[\pi(2h+k)],$$

and the interaction distances for the four exchange parameters are the following:

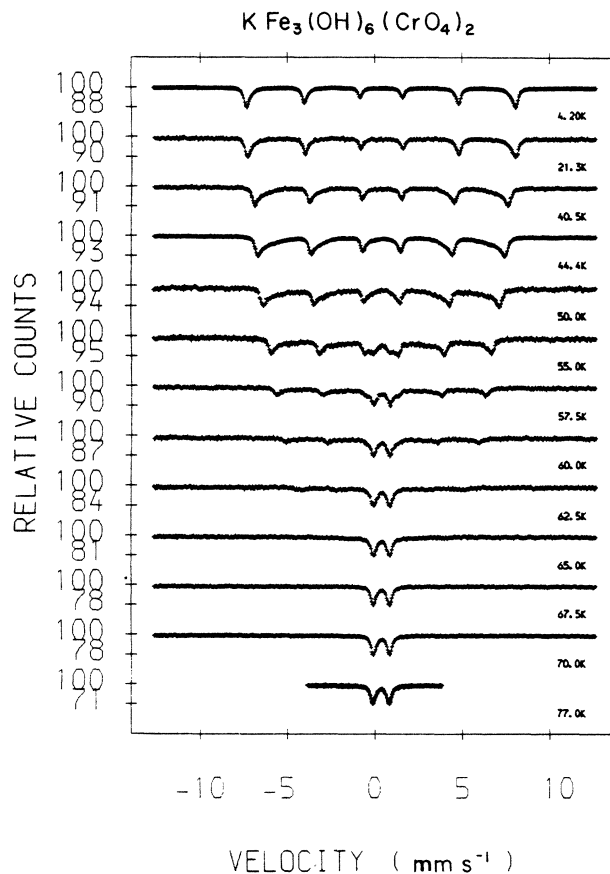


FIG. 7. Mössbauer spectra of $\text{KFe}_3(\text{OH})_6(\text{CrO}_4)_2$ as a function of temperature.

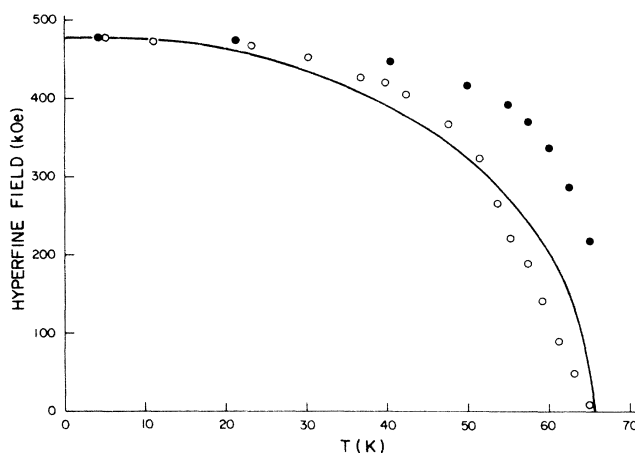


FIG. 8. Magnetic-hyperfine field (\bullet) as a function of temperature for $\text{KFe}_3(\text{OH})_6(\text{CrO}_4)_2$. Also shown (\circ) are the weak spontaneous magnetic moments recorded for $\text{KFe}_3(\text{OH})_6(\text{CrO}_4)_2$ below T_N , with $M(0)$ normalized to the value of the magnetic-hyperfine field at 0 K. Fit to a Brillouin curve with $S = \frac{5}{2}$ indicated.

$$J_1 = \frac{a}{2},$$

$$J_2 = \frac{\sqrt{3}a}{2},$$

$$J_3 = a,$$

$$J_4 = a.$$

For a spin propagation vector $\mathbf{k}=(0,0,l)$, where $l=0$ or $\frac{1}{2}$, the experimentally observed mode $\zeta(k)$ is diagonalized by the matrix

$$Q = \begin{pmatrix} 1 & 1 & 1 \\ 1 & c & c^* \\ 1 & c^* & c \end{pmatrix},$$

with $c = \exp(2\pi i/3)$.

The three columns Q_1 , Q_{11} , and Q_{111} are connected to the unitary spin σ_j by

$$\sigma_j = \frac{1}{2}(\xi + i\eta)Q_j + \text{c.c.},$$

where ξ and η are two vectors at right angles. The solution $Q_1=(1,1,1)$ corresponds to a ferromagnetic mode with

$$\lambda_1 = 2J_3 + 4J_4 + 4J_1 + 4J_2.$$

The solutions Q_{11} and Q_{111} belong to a triangular-spin mode with

$$\lambda_{11,111} = 2J_3 + 4J_4 - 2J_1 - 2J_2.$$

For $Q_{11}=(1,c,c^*)$ the inverse Fourier transformation yields

$$\sigma_1 = \xi,$$

$$\sigma_2 = \xi \cos\left(\frac{2\pi}{3}\right) - \eta \sin\left(\frac{2\pi}{3}\right),$$

$$\sigma_3 = \xi \cos\left(\frac{2\pi}{3}\right) + \eta \sin\left(\frac{2\pi}{3}\right).$$

In the degenerate mode Q_{111} , σ_2 and σ_3 are interchanged. It is easily verified that

$$\sigma_1 + \sigma_2 + \sigma_3 = 0,$$

i.e., the spins are in a triangular configuration in this mode. The directions of ξ and η are not specified by this treatment.

The stability conditions of the calculated modes follow from the condition that $\lambda(k)$ must be a maximum. Thus

$$\frac{\partial \lambda}{\partial h} = \frac{\partial \lambda}{\partial k} = 0, \quad \frac{\partial^2 \lambda}{\partial h^2} \leq 0, \quad \begin{vmatrix} \frac{\partial^2 \lambda}{\partial h^2} & \frac{\partial^2 \lambda}{\partial h \partial k} \\ \frac{\partial^2 \lambda}{\partial h \partial k} & \frac{\partial^2 \lambda}{\partial k^2} \end{vmatrix} \geq 0.$$

For the antiferromagnetic triangular mode these conditions are the following:

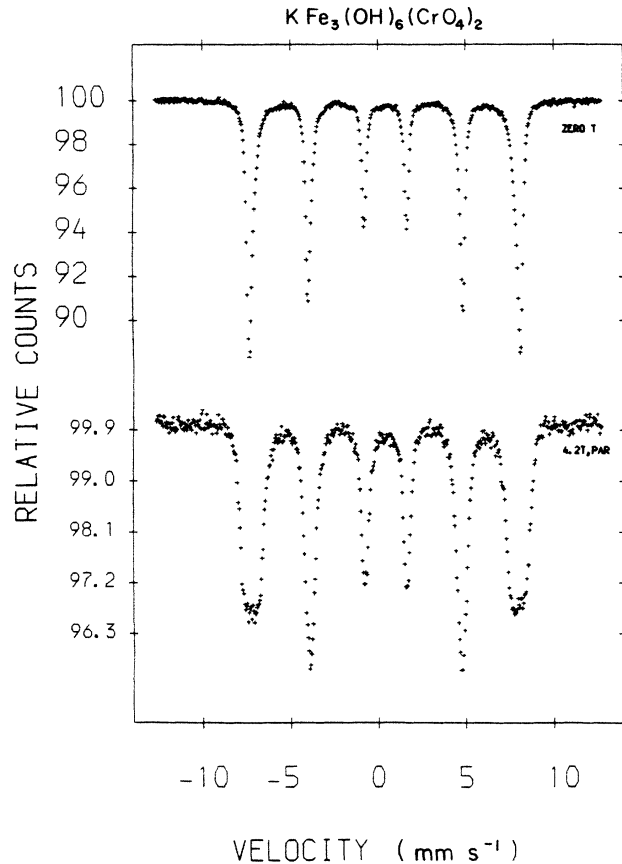


FIG. 9. Mössbauer spectra of $\text{KFe}_3(\text{OH})_6(\text{CrO}_4)_2$ at 4 K in (a) zero magnetic field and (b) in an external longitudinal, magnetic field of 42 kOe.

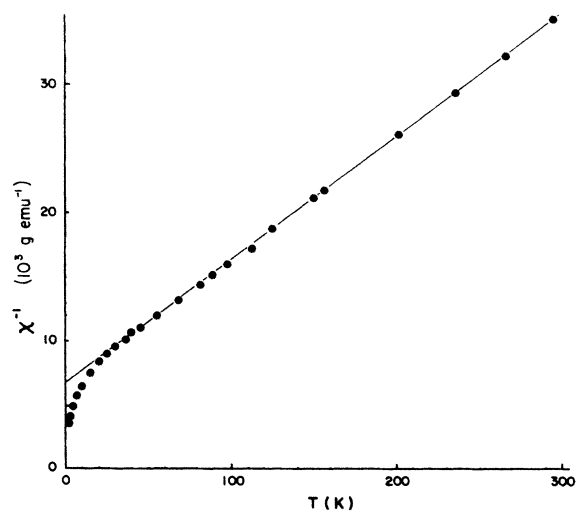


FIG. 10. Reciprocal magnetic susceptibilities of $\text{KCr}_3(\text{OH})_6(\text{CrO}_4)_2$ as a function of temperature. The linear part of the curve is fitted to a Curie-Weiss law, $\chi = C/(T - \Theta)$, where $\Theta = -67.5$ K and the effective moment of Cr^{3+} , P_{eff} , is equal to $3.7\mu_B$.

$$J_1 + J_2 - 8J_4 \leq 0, \quad J_1(J_3 + J_2) + J_2(J_3 + 3J_2) + J_4(-8J_3 - 15J_2 + J) \geq 0.$$

The largest integral J_1 , acting through a distance of $a/2$ in the kagome plane via a $\text{Fe}^{3+}-\text{OH}-\text{Fe}^{3+}$ 134° bond angle, is expected to be negative¹⁷ and if in $\text{KFe}_3(\text{OH})_6(\text{SO}_4)_2$ it dominates, one predicts the experimentally observed triangular mode. However, as discussed later, J_2 , J_3 , and J_4 may make a more significant contribution in $\text{KCr}_3(\text{OH})_6(\text{SO}_4)_2$.

In the ferromagnetic mode the stability conditions are the following:

$$J_1 + J_2 + 4J_4 \geq 0, \quad J_1(J_3 + 2J_2) + J_2J_3 + J_4(2J_4 + 4J_3 + 5J_2 + J_1) \geq 0.$$

Spin configurations other than $\mathbf{k}=(0,0,0)$ could also be considered leading to other types of solutions such as helical waves. Study of jarosites in external magnetic fields would be of interest: In the honeycomb lattice such experiments lead to soliton and vortex formation.¹⁸

In principle the above method could be extended to the three kagome planes of a hexagonal unit cell leading to a 9×9 matrix. However, as pointed out earlier, interplanar magnetic exchange should be very weak. Regnault¹⁸ used a perturbation method for the honeycomb plane where there are only two Bravais lattices, as compared to the three Bravais lattices of the kagome plane.

V. DISCUSSION

Triangular-spin magnetic structures are predicted for $\text{KFe}_3(\text{OH})_6(\text{SO}_4)_2$ and $\text{KFe}_3(\text{OH})_6(\text{CrO}_4)_2$ by the matrix method taking into account the dominant, antiferromagnetic superexchange through $134^\circ \text{Fe}^{3+}-\text{O}-\text{Fe}^{3+}$ bond angles in the kagome plane.

Evidently, from the magnetic structure (Figs. 5 and 6), correlation occurs between spins in adjacent kagome planes 6.3 Å apart. The weak interplane magnetic exchange, which acts through a chain of nonmagnetic ions $-\text{OH}-\text{K}-\text{OH}-$, or $-\text{O}-\text{S}-\text{O}-\text{OH}-$ and the strong magnetic exchange in the plane should lead to planar-spin correlations. These are indicated in the neutron diffraction pattern of $\text{KFe}_3(\text{OH})_6(\text{SO}_4)_2$. The $(1,0, \frac{1}{2})$ reflection is broadened even at 10 K and its width increases with increasing temperature. A broad peak persists even at 80 K, above the Néel temperature of 46 K. Short-range magnetic order of this nature is expected in planar magnetic materials.¹⁹ The $(1,0, \frac{1}{2})$ reflections at 10 K in $\text{KFe}_3(\text{OH})_6(\text{SO}_4)_2$ and in $\text{PbFe}_6(\text{OH})_{12}(\text{SO}_4)_4$ appear to be broader than the $(1,0, \frac{1}{2})$ reflection in $\text{TlFe}_3(\text{OH})_6(\text{SO}_4)_2$.

The values of T_c/Θ for $\text{KFe}(\text{OH})_6(\text{SO}_4)_2$ and $\text{KFe}_3(\text{OH})_6(\text{CrO}_4)_2$ are very low (≈ 0.1) and the value appears to be even lower for $\text{KCr}_3(\text{OH})_6(\text{SO}_4)_2$. The low magnitude for T_c/Θ indicates planar magnetic ordering. However, the values of T_c/Θ are less than those predicted by most models of planar systems¹⁹ and hence magnetic exchange energies evaluated from T_c are considerably lower than those evaluated from Θ .

The value of the Curie-Weiss constant for $\text{KCr}_3(\text{OH})_6(\text{SO}_4)_2$, $\Theta = -67.5$, yields an approximate magnetic exchange interaction, $J_2 = -2.8$ K and hence the curve in the plot of χ^{-1} versus T below 20 K, Fig. 10, most likely reflects magnetic ordering at $\approx 1-2$ K. For a more precise estimate of J , the susceptibilities require fitting to a high-temperature expansion evaluated for the kagome lattice. No magnetic neutron-diffraction data have

yet been recorded for $\text{KCr}_3(\text{OH})_6(\text{SO}_4)_2$ because of the extremely low ordering temperature but the negative sign of Θ shows that the principal magnetic coupling is antiferromagnetic and implies a triangular-spin mode rather than a ferromagnetic mode. From the relative Néel temperatures we can conclude that the magnetic exchange energy in $\text{KCr}_3(\text{OH})_6(\text{SO}_4)_2$ is smaller by more than 1 order of magnitude than the magnetic exchange energy in $\text{KFe}_3(\text{OH})_6(\text{SO}_4)_2$ and $\text{KFe}_3(\text{OH})_6(\text{CrO}_4)_2$.

The principal magnetic exchange interaction in jarosites is superexchange through $134^\circ \text{Cr}^{3+}-\text{OH}-\text{Cr}^{3+}$ and $\text{Fe}^{3+}-\text{OH}-\text{Fe}^{3+}$ bonds in the kagome plane. Interestingly, the magnetic superexchange couplings (J'_4) for $133^\circ \text{Cr}^{3+}-\text{O}-\text{Cr}^{3+}$ and $132^\circ \text{Fe}^{3+}-\text{O}-\text{Fe}^{3+}$ bonds in Cr_2O_3 and Fe_2O_3 , respectively, as determined from inelastic neutron scattering, show a parallel trend: $J'_4 = 0.2 \pm 2.3$ K in Cr_2O_3 and $J'_4 = -23.2 \pm 1.0$ in Fe_2O_3 (Refs. 20 and 21). The sign of the superexchange for Cr^{3+} is ambiguous.^{20,22} Superexchange interaction is much stronger in $132^\circ \text{Fe}^{3+}-\text{O}-\text{Fe}^{3+}$ bonds than in $\text{Cr}^{3+}-\text{O}-\text{Cr}^{3+}$ bonds because of π bonding of e_g electrons in $\text{Fe}^{3+}(t_{2g}^3 e_g^2)$ as compared to $\text{Cr}^{3+}(t_{2g}^3)$.¹⁷

In $\text{KCr}_3(\text{OH})_6(\text{SO}_4)_2$, J_2 and J_3 occur through Cr^{3+} -anion-anion- Cr^{3+} interaction and such coupling can be stronger than 133°Cr^{3+} -anion- Cr^{3+} magnetic interaction.²⁰ Hence, the principal antiferromagnetic ordering implied by the negative sign of Θ in the magnetic susceptibilities of $\text{KCr}_3(\text{OH})_6(\text{SO}_4)_2$ may result from a combination of terms in the energy eigenvalue, $\lambda_{11,11} = 2J_3 + 4J_4 - 2J_1 - 2J_2$.

The weak ferromagnetic moment [$0.03\mu_B/(\text{Fe atom})$] of $\text{KFe}_3(\text{OH})_6(\text{CrO}_4)_2$ vanishes above about the same temperature ($T_N = 65$ K) as the three-dimensional antiferromagnetism and therefore the moment is most probably not caused by a second phase. However, this does not necessarily signify a weak parasitic ferromagnetic moment arising from canting of the antiferromagnetically coupled spins: effects of nonstoichiometry in the $\text{KFe}_3(\text{OH})_6(\text{CrO}_4)_2$ lattice cannot be ruled out. In this connection it is interesting to note that no weak moment is observed in $\text{KFe}_3(\text{OH})_6(\text{SO}_4)_2$ where the magnetic unit cell is double that of the chemical unit cell in the c -axis direction. A canted moment should not occur in our model of the magnetic structure of $\text{KFe}_3(\text{OH})_6(\text{SO}_4)_2$ (Fig. 5), since the spins are reversed in the two halves of the magnetic unit cell; hence any resultant spontaneous moment, a vector quantity, would be zero. On the other hand, a spontaneous moment is permitted in the intrinsic $\text{KFe}_3(\text{OH})_6(\text{CrO}_4)_2$ magnetic unit cell from symmetry considerations whether the crystallographic space group is taken to be $R\bar{3}m$ or $R3m$. The magnetic symmetry, Fig.

6, is low: The magnetic crystal class is 1 and a spontaneous moment either parallel to *c* or perpendicular to *c* would be allowed in $\text{KFe}_3(\text{OH})_6(\text{CrO}_4)_2$ for the spins lying perpendicular to the *c* axis.

The temperature dependence of the weak moment in $\text{KFe}_3(\text{OH})_6(\text{CrO}_4)_2$ differs from that of the magnetic-hyperfine field, Fig. 8. The magnetic-hyperfine field should reflect the magnetization at Fe^{3+} ; if the moment were to arise from canting, noncoincidence of the two curves would signify some temperature dependence in canting angle. It should be noted that a weak spontaneous moment has been reported previously in $\text{KFe}_3(\text{OH})_6(\text{CrO}_4)_2$ at temperatures below 73 K by Powers *et al.*²³

In the Mössbauer spectra of $\text{KFe}_3(\text{OH})_6(\text{CrO}_4)_2$, at temperatures between 40.5 and 55 K, the four outside lines of the magnetic sextet are broadened asymmetrically (Fig. 7). It is not clear at present if this represents a phase transition in this temperature range or some type of dynamic effect. The magnetic susceptibilities in this temperature range show no evidence for a phase transition.

ACKNOWLEDGMENT

M.G.T. thanks E. F. Bertaut and members of Laboratoire de Crystallographie for their kind hospitality and for many stimulating discussions during the tenure of a France-Canada exchange.

*At Laboratoire de Crystallographie, Centre National de la Recherche Scientifique, Grenoble during part of this work.

¹J. E. Dutrizac and S. Kaiman, *Can. Mineral.* **14**, 151 (1976).

²J. Kubisz, *Mineral. Pol.* **1**, 47 (1970).

³A. Bonnin and A. Lecerf, *C. R. Acad. Sci. Paris* **262**, 1782 (1966).

⁴S. Menchetti and C. Sabelli, *Neues Jahrb. Mineral. Monatsh.* **1976**, 406 (1976).

⁵R. Wang, W. F. Bradley, H. Steinfink, *Acta Crystallogr.* **18**, 249 (1965).

⁶J. Szymanski, *Can. Mineral.* (to be published).

⁷I. Syôzi, *Prog. Theor. Phys.* **6**, 306 (1951).

⁸M. Takano, T. Shinjo, M. Kiyama, and T. Takada, *J. Phys. Soc. Jpn.* **25**, 902 (1968).

⁹M. Takano, T. Shinjo, and T. Takada, *J. Phys. Soc. Jpn.* **30**, 1049 (1971).

¹⁰A. M. Afanasev, V. D. Gorobchenko, D. S. Kulgawczuk, and I. I. Lukashevich, *Phys. Status Solidi* **26**, 697 (1974).

¹¹A. Leclerc, *Phys. Chem. Minerals* **6**, 327 (1980).

¹²J. Dutrizac (unpublished).

¹³M. F. Collins (private communication).

¹⁴W. B. Muir and J. Addison (unpublished).

¹⁵E. Hermon, R. Haddad, D. J. Simkin, D. E. Brardao, and W. B. Muir, *Can. J. Phys.* **54**, 1149 (1976).

¹⁶E. F. Bertaut, in *Magnetism*, edited by G. T. Rado and H. Suhl (Academic, New York, 1963), Vol. 3.

¹⁷J. B. Goodenough, *Magnetism and the Chemical Bond* (Interscience, New York, 1963).

¹⁸L. P. Regnault, Ph.D. thesis, Université de Grenoble, 1981.

¹⁹L. J. de Jongh and A. R. Miedema, *Adv. Phys.* **23**, 1 (1974).

²⁰E. J. Samuelsen, M. T. Hutchings, and G. Shirane, *Physica* **48**, 13 (1970).

²¹E. J. Samuelsen and G. Shirane, *Phys. Status Solidi* **42**, 241 (1970).

²²W. P. Osmond, *Proc. Phys. Soc.* **79**, 394 (1962).

²³D. A. Powers, G. R. Rossman, H. J. Schuger, and H. B. Gray, *J. Solid State Chem.* **13**, 1 (1975).